

# American Chemical Science Journal 3(2): 151-163, 2013



SCIENCEDOMAIN international www.sciencedomain.org

# Characterization of Plasma Sprayed Pure Red Mud Coatings: An Analysis

Alok Satapathy<sup>1</sup>, Harekrushna Sutar<sup>2\*</sup>, Subash Chandra Mishra<sup>2</sup> and Santosh Kumar Sahoo<sup>2</sup>

<sup>1</sup>Mechanical Engineering Department, National Institute of Technology, Rourkela, India. <sup>2</sup>Metallurgical and Materials Engineering Department, National Institute of Technology, Rourkela, India.

#### Authors' contributions

This work was carried out in collaboration between the authors. Author AS carried out the experimental work supervised by author SCM. Author HS collected the data and did editing and write-up of manuscript. Author SKS supported technically for completion of project successfully. All authors read and approved the final manuscript.

Research Article

Received 9<sup>th</sup> February 2013 Accepted 13<sup>th</sup> March 2013 Published 23<sup>rd</sup> March 2013

# **ABSTRACT**

The characteristics of plasma sprayed pure red mud coatings have been investigated. The red mud was collected as a waste from aluminium production. In order to understand the coating characteristics, pure red mud was plasma coated. After plasma spraying, the coated materials have been subjected to series of tests to determine coating thickness, adhesion strength, micro structural characterization of cross section, X-ray diffraction and coating deposition efficiency. Plasma spraying is done at 200, 250, 300 and 400 ampere current. Torch input power is maintained at 6,9,12 and 16 kW. The coating samples chose are dimension 50mm×25mm×2mm. Available substrates are made of aluminium, copper, mild steel and stainless steel.

Keywords: Plasma spraying; red mud coating; coating characteristics.

#### 1. INTRODUCTION

Surface modification is a generic term now applied to a large field of diverse technologies that can be gainfully harnessed to achieve increased reliability and enhanced performance of industrial components. Surface modification has come up in the last two decades or so to describe interdisciplinary activities aimed at tailoring the surface properties of engineering materials. The objective of surface engineering is to upgrade their functional capabilities keeping the economic factors in mind [1]. Surface engineering is the name of discipline, and surface modification is the philosophy behind it.

Coating technologies have advanced a lot during the last decades, and it is now possible to deposit films with a great variety of properties. Plasma spray is one of the most widely used techniques of surface treatment due to its great versatility and its application to wide spectrum of materials. The hard coatings used to protect against wear are commonly made of nickel, iron, cobalt, ceramics [2-3]. The behavior of a coated surface is controlled by geometry of contact, the material characteristics and finally the operational parameters [4]. The unique control of microstructure led to the production of materials with enhanced or novel behavior concerning their magnetic [5], electrical [6-7], optical [8-10] and mechanical [11-12] properties.

Plasma spraying is often considered as a potential alternative to traditional coating manufacturing techniques (such as hard chrome electroplating) for production of wear resistant coatings [13-16].

The present investigation focuses on characteristics of red mud. Red mud emerges as the major waste material during production of alumina from bauxite by the Bayer's process. It comprises of oxides of iron, Titanium, aluminium and silica along with some other minor constituents. To explore the coating potential of this industrial waste is in progress. Reducing wear to a minimum and saving the cost of replacing worn failure machine element is very important in industry. Ceramic materials, owing to their high hardness and chemical inertness, have received much attention for their high resistance to wear, corrosion and high temperature oxidation [17]. The high cost in production and their brittle character, however will restrict the application of ceramics in industry to a certain extent. For such reason, coatings onto materials which are cheap and reliable in shock are in important.

# 2. EXPERIMENTAL

In this study pure red mud as powder is used as raw material for coating on various substrates. The red mud is collected from the alumina plant of National Aluminium Company (NALCO) located at Damonjodi in the state of Orissa, India. The chemical composition of red mud is specified in Table 1. The received powder is sieved to obtain particles in the size range of  $80\text{-}100~\mu\text{m}$ .

Table 1. Chemical analysis of red mud

Constituents	$Al_2O_3$	TiO <sub>2</sub>	Na₂O	$P_2O_5$	Ga <sub>2</sub> O <sub>3</sub>	Zn	С	Fe <sub>2</sub> O <sub>3</sub>	SiO <sub>2</sub>	CaO	$V_2O_5$	Mn	Mg
Wt.%	15	3.7	4.8	0.67	0.096	0.018	0.88	54.8	8.44	2.5	0.38	1.1	0.056

Substrates used in the present study are made of aluminium, copper, mild steel and stainless steel having dimension of 50mm×25mm×2mm. The specimens are grit blasted at pressure of 3 kg/cm² using alumina grits having a grit size of 60. The standoff distance in

short blasting is kept between 120-150mm. The average roughness of the substrates is 6.8 µm. The grit blasted specimens are then cleaned in an ultrasonic cleaning unit for at least 10 minutes. Spraying is carried out immediately after cleaning. The spraying is done using conventional atmospheric plasma spraying (APS) set up, a direct current type and produced byThermacut USA. The plasma input power is varied from 6 to 16 kW by controlling the gas flow rate, voltage and the arc current at 10 g/min, using a turntable type volumetric powder feeder. The Powder Feeder is a mass flow controlled powder feeder produced by AMT AG. The schematic diagram of plasma spraying equipment is shown in Fig. 1.

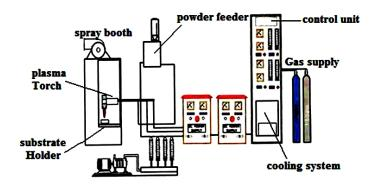


Fig. 1. Arrangement of the plasma spraying equipment

Spraying is done at a spraying angle of 90°. The powder feeding is external to the gun with feeding distance 120 mm. The properties of coatings are dependent on the spray process parameters. The operating parameters during coating deposition are listed in Table 2.

Table 2. Operating parameters during coating deposition

Operating parameters	Values			
Plasma Arch Current(ampere)	200, 250, 300, 400			
Arc Voltage ,Volt	30,36,40			
Torch Input Power, kW	6,9,12,16			
Plasma Gas ,Argon, Flow rate, Ipm	20			
Secondary gas ,Nitrogen, Flow rate, Ipm	2			
Carrier gas , Argon, flow rate, lpm	7			
Powder Feed Rate, g/min	10			
Torch to Base distance ,TBD,mm	100			

# 3. CHARACTERIZATION OF COATINGS

# 3.1 Coating Thickness Measurement

Thickness of the red mud coatings on different substrates are measured on the polished cross sections of the samples, using an optical microscope. Five readings are taken on each specimen and the average value is reported as the mean coating thickness.

# 3.2 X-Ray Diffraction Studies

The coatings are examined for the identification of the crystalline phases with a Philips X-Ray diffractometer. The X-Ray diffractograms are taken using Cu Kα radiation.

# 3.3 Scanning Electron Microscope (SEM) Studies

Specimens of the size 10mm×13mm×5mm are sliced from the coated samples for SEM observation. Cross sections of the specimens are observed in scanning electron microscope Jeol-T-330 mostly using the secondary electron imaging. Coating cross sections are polished in 3 stages using silicon carbide abrasive papers of reducing grit sizes and then with diamond pastes on a wheel for coating interface analysis under SEM.

# 3.4 Coating Deposition Efficiency

Deposition efficiency is defined as the ratio of the weight of coating deposited on the substrate to the weight of the expended feedstock. Weighing method is accepted widely to measure this. Each specimen is weighed before and after coating deposition. The difference is the weight ( $G_c$ ) of coating deposited on the substrate. From the powder feed rate and time of deposition the weight of expended feed stock ( $G_p$ ) is determined. The deposition efficiency ( $\eta$ ) is then calculated using the following equation [18].

 $\eta = (G_c/G_c)X 100 \%$ 

Weighing of samples is done using a precision electronic balance within 0.1 mg accuracy.

# 3.5 Evaluation of Coating Adhesion Strength

To evaluate the coating adhesion strength, a special type jig is fabricated. Cylindrical mild steel dummy samples (length 25 mm, top and bottom diameter 9.5 mm) are prepared. The surfaces of the dummies are roughened by punching. These dummies are then fixed on top of the coating with the help of a polymeric adhesive (epoxy 900-C) and pulled with tension after being mounted on the jig. The coating pullout test is carried out using the set up Instron 1195 at a crosshead speed of 10 m/minute.



Fig. 2. Adhesion test set up Instron 1195

The moment coating gets torn off from the specimen, the reading (of the load), which corresponds to the adhesive strength of the coating, is recorded. A typical test set up during testing is shown in Fig. 2. The test is performed as per ASTM C-633.

#### 4. RESULTS AND DISCUSSION

#### 4.1 Coating Thickness

To ensure coat ability of red mud on different substrates, coating thickness was measured on polished cross section of the samples. The thickness values obtained for coatings deposited at different power levels for Al, Cu, MS and SS substrates are presented in Fig. 3. Maximum coating thickness of  $\sim 200$  micron on aluminium,  $\sim 210$  micron on copper,  $\sim 190$  micron on mild steel and  $\sim 170$  micron on stainless steel substrates are obtained. From the figure it is evident that there is an increase in coating thickness with increase in input power to plasma torch; up to about 12 kW and then for further higher input power , no improvement in coating thickness is reported.

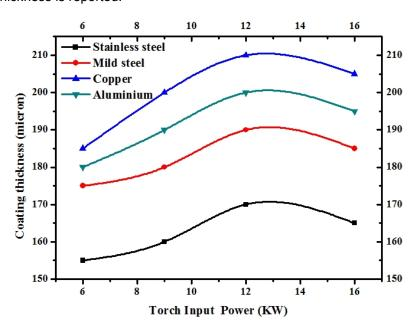


Fig. 3. Thickness of red mud coatings made at different power level

It is also seen from the Fig. 3 that there is difference in thickness obtained for different substrates. Coating thickness is higher for copper than that of aluminium, mild steel or stainless steel substrates, at all power level. This difference is attributed to thermal conductivity of the substrate material, i.e. for materials with higher conductivity (i.e. aluminium and copper) ,the heat transfer from the sprayed particles occurs at a faster rate than in case of materials with relatively lower conductivity(i.e. MS, SS). This might be enhancing the deposition rate and hence the coating thickness.

# 4.2 Adhesion Strength

From the microscopic point of view, adhesion is due to physio-chemical surface forces, which can be established at the coating substrate interface [19] and corresponds to the work of adhesion. In the present study it is found that in all samples fracture occurred at the coating substrate interface. The results obtained for red mud coatings are tabulated in Table. 3.

Coating	Arc current,	Arc Voltage,	Torch input	Adhesion strength MPa			
material	ampere	volt	power kW	Al	Cu	MS	SS
	200	30	6	6.39	5.64	4.65	4.63
Red mud	250	36	9	6.92	6.53	6.43	5.87
	300	40	12	5.76	6.69	7.75	6.12
	400	40	16	3 67	3.11	7 54	3 85

Table 3. Coating adhesion strength at different spraying condition

The variation of interface adhesion strength of red mud coatings on different substrates with operating power level of the plasma torch are presented in Fig. 4. Maximum adhesion strength of 7.75 MPa is recorded for mild steel substrate.

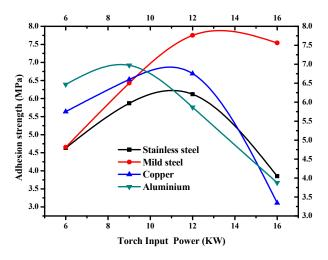


Fig. 4 Adhesion Strength of red mud coatings made at different power level on different substrates

The influence of torch input power on coating adhesion is evident from the Fig. 4. For coating on aluminium substrate, the strength has increased from 6.39 MPa to 6.92 MPa with increase in operating power from 6 kW to 9 kW. Coating deposited beyond 9 kW operating power exhibited a detrimental effect on adhesion strength. Similarly, maximum coating adhesion strengths of 6.69 MPa at 12 kW, 7.75 MPa at 12 kW and 6.12 MPa at12 kW have been reported for copper, mild steel and stainless steel substrates respectively. It is noted that invariably in all cases the interface bond strength increases with the input power of the torch up to a certain power level and then shows a decreasing trend in coating adhesion.

Initially, when the operating power level is increased, the melting fraction and velocity of the particles also increases .Therefore there is better splashing and mechanical interlocking of molten particles on the substrate surface leading to increase in adhesion strength. But, at much higher power level, the amount of fragmentation and vaporization of the particles increase. There is also greater chance of smaller particles to fly off during spraying. This results in poor adhesion strength of the coatings.

# 4.3 Coating Surface and Interface

The coating substrate interface plays the most important role on adhesion of the coating. The polished cross-sections of the samples are examined under SEM. The microstructures of coatings on aluminium substrates are shown in Fig. 5. (a), (b), (c) and (d). Comparing these Figures it can be seen that the morphology is more homogeneous for the coating deposited at 12 kW. In case of coatings deposited at lower power level, some un-melted particles are seen with large amount of cavitations. Cavities are also seen along the interface for the coatings deposited at 6 kW and 16 kW which might have resulted poor adhesion of coating, with a difference that, no un-melted particles are found at higher power level of coating deposition. At 16 kW power level cracks are developed along the coating layers which has deteriorated the coating homogeneity.

Cracks are observed along the coating substrate interface; may be due to mismatch of thermal expansion coefficient of substrate and coating materials, resulted in lowering adhesion strength. Although some pores are observed (Fig. 5c) those are spherical in shape and have helped in increasing the adhesion strength and longitudinal cracks observed at the inter particle layers at 16 kW, reduces the adhesion strength.

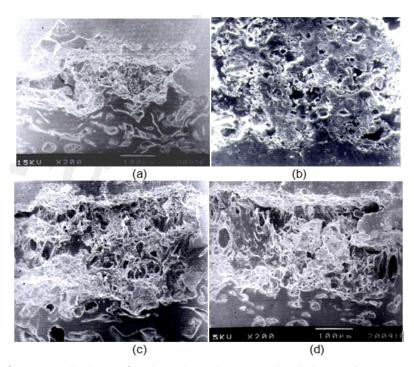


Fig. 5. Interface morphology of red mud coatings on aluminium substrates at (a) 6 kW (b) 9kW (c) 12 kW (d) 16 kW operating power level

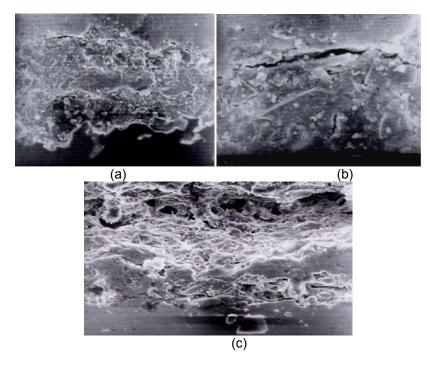


Fig. 6. Interface morphology of red mud coatings deposited at 12 kW power level on (a) copper, (b) mild steel (c) stainless steel substrates

The coating interface morphology of red mud coatings deposited at 12 kW for different substrates as shown in Fig. 6. (a), (b) and (c). Comparing these Figures, it is seen that there is no cavity formation along the coating substrate interface for coatings made on copper substrate. But some cracks are visible along the interface boundary in case of steel substrates. Cavity formation along the coating layers is observed in stainless steel substrates. However copper substrate shows better homogeneity in the coating. The crack or cavity formation at the boundaries may also be the cause of difference in interface adhesion strengths of coatings on different substrate.

# 4.4 XRD Phase Composition Analysis

To ascertain the phases present and phase changes taking place during plasma spraying, the X-ray diffractograms are taken on the raw material and the coatings at different operating power level. The XRD results are shown in Fig. [7-9].

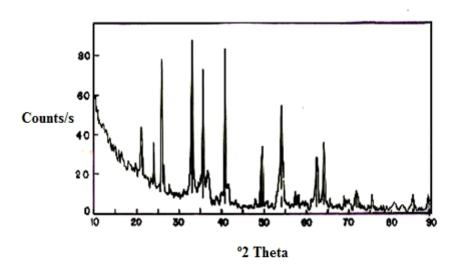


Fig. 7. X-ray diffractogram of red mud collected from NALCO

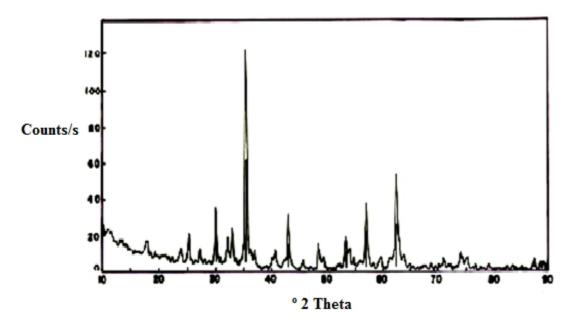


Fig. 8. X-Ray diffractogram of red mud coating deposited at 6 kW Operating power level

From the diffractograms it is seen that the major constituents present in the red mud are hematite ( $Fe_2O_3$ ), anatese / rutile / brookite ( $TiO_2$ ) and silica. Presence of silica in amorphous form is well visualized in Fig. 7. During plasma spraying some of the amorphous (silica) has transformed to crystalline forms. Transformation of hematite is also observed. As marked in Fig. 9(c), probably MgO and  $Fe_2O_3$ have formed a compound MgFe<sub>2</sub>O<sub>4</sub>. Some of the diffraction peaks found to be absent in coatings as compared to the raw material. This

may be due to vaporization of oxides of alkali and alkaline earth metals (CaO, MgO etc.) from the raw material as well as due to formation of complex oxides such as  $MgFe_2O_4$ .

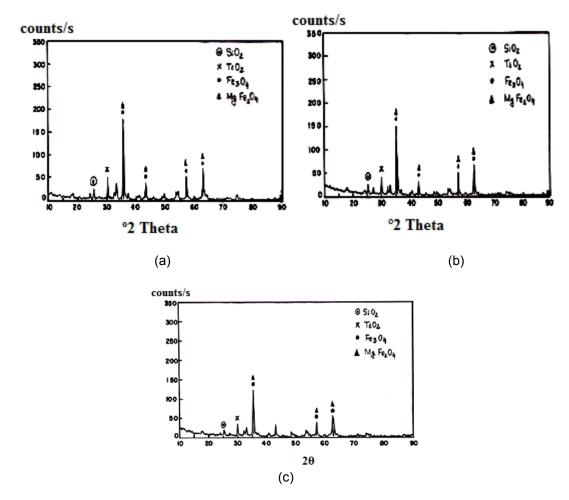


Fig. 9. X-Ray diffractogramof red mud coatings deposited at (a) 9 kW (b) 12 kW (c) 16 kW operating power level

It can be visualized from Fig. [8-9] that, glassy (silica) phase, which is observed in the raw material (Fig. 7) is not found in the coated samples. This may be due to the fact that, at high temperature amorphous silica has transformed to crystalline phases.

# 4.5 Coating Deposition Efficiency

In this work, torch input power is selected as the parameter to investigate its influence on deposition of powders taken on all the four substrates. Fig. 10 presents the variation of deposition efficiency with operating power level on the substrates for red mud coating. It is interesting to note that the deposition efficiency, in all cases, is increased in a sigmoidal fashion with the torch input power. For example: on aluminium substrates, the value increases from 7.2% to 23.59% (with input power to plasma torch increasing from 6 kW to 16 kW) for red mud deposition. Whereas, when this material is deposited on copper substrates,

the efficiency of deposition is seen to vary from 7% to 24 %. The results obtained for red mud are presented in Table4.

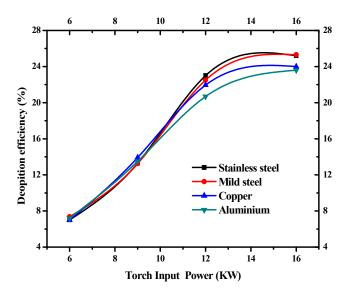


Fig. 10. Deposition efficiency of red mud coatings made at different power level at different substrates

Table 4. Coating deposition efficiency at different spraying conditions

Coating material	Arc	Arc	Torch input	Deposition efficiency%				
	current, ampere	voltage, volt	power kW	Al	Cu	MS	SS	
	200	30	6	7.2	7	7.35	7	
Red Mud	250	36	9	13.5	13.92	13.25	13.3	
	300	40	12	20.68	21.95	22.5	23	
	400	40	16	23.59	24	25.3	25.2	

It reveals that efficiency of coating deposition is significantly influenced by the input power of the torch. Fig. 10. shows the variation of deposition efficiency of red mud coating. Plasma spray deposition efficiency of a given material depends on its melting point, thermal heat capacity and particle size of the powder etc. At lower power level, the plasma jet temperature is not high enough to melt the entire feed powder (particles) that enter the plasma jet. As the power level is increased, the average plasma temperature increases, thus melting a larger fraction of the feed powder. The spray efficiency therefore increases with increase in input power to the plasma torch. However, beyond a certain power level of the torch, temperature of the plasma becomes high enough leading to vaporization/dissociation of the powder particles. Thus there is not much increase in deposition efficiency and coating thickness as well. However, the operating power above which the efficiency decrease depends on the chemical nature of the feed material i.e. powder and its particle size, thermal conductivity, in-situ phase transformations etc. The trend of variation is similar for all substrates and in case of all coating materials considered in this work.

#### 5. DISCUSSION & CONCLUSION

Sutar et al. [20] studied that red mud the waste generated from alumina plants is eminently coat able on metal substrates employing thermal plasma spraying technique. Coatings made with red mud posses desirable coating characteristics and have ample resistance to wear. Therefore, red mud can be a substitute for conventional plasma spayed ceramic coatings. Coatings made with red mud posses desirable coating characteristics such as good adhesion strength, comparable to those of other conventional plasma sprayed ceramic coatings. Deposition efficiency of 25% is obtained for red mud coatings. Coating morphology for red mud is largely affected by the torch input power. During plasma spraying of red mud, phase transformation and inter oxide formation are observed. Evaluation of thermal stability of these coatings may be done to find high temperature applications. Sliding wear behavior under different operating condition was investigated by Prasad et al. [21] to identify suitable application areas. Post heat treatment of these coatings may also be done to study further improvement in coating qualities and properties. Operating power level of plasma torch influences the coating adhesion strength. The coating interfacial morphology is also largely affected by the torch input power. Due to phase transformations of the oxides formed during plasma spraying, changes in the coating characteristics are observed. Spraying parameters such as plasma arc current, torch input power, and surface roughness of the substrate significantly affect the efficiency of coating deposition. It is evident that with an appropriate choice of processing conditions a sound and adherent ceramic coating is achievable using industrial waste like red mud.

#### **ACKNOWLEDGEMENTS**

Authors HS and SKS are obliged to professor (Dr.) AlokSatapathy of Mechanical engineering department and Professor (Dr.) Subash Chandra Mishra of Metallurgical and Materials Engineering department of National Institute of Technology, Rourkela, Odisha, India.

# **COMPETING INTERESTS**

Authors have declared that no competing interests exist.

#### **REFERENCES**

- Heiman RB. Plasma spray coatings Principle and Application, VCH, Weinheim, Germany: 1996.
- 2. Kushner BA, Novinski ER. Thermal spray coatings, ASM Handbook. 1992;18(ASM):829-833.
- Crook P. Friction and wear of Hard facing Alloy, ASM Handbook. 1992;18(ASM):758-765.
- 4. Holmberg K, Mathews A, Ronkainen H. Tribol. Int. 1998;31(1-3):107-120.
- Terakura K. In: ShinjoT andTakada T (Eds.), Metalic superlatices, Elsvier, Amsterdam. 1987:223-232.
- 6. Matijasevic V, Beasley MR. In: Shinjo T, Takada T (Eds), Metalic superlatices, Elsvier, Amsterdam. 1987;187.
- 7. Falco M, Schuller IK. In: Chang LL, Giessen BC; (Eds). Synthetic Modulated Structures, Academic Press, New York. 1985;257.

- 8. Holonyak N Jr, Hess K. In: ChangL. L, Giessen B.C (Eds), Synthetic Modulated Structure, Academic press, New York. 1985;257.
- 9. Spiller E, Segmuller E, Rife J, Haelbich RP. Appl. Phys. Lett. 1980;(37);1048.
- 10. Underwood H, Barbee TW. Nature. 1981;(194):492.
- 11. Koehler S, Phy. Rev. B2. 1970;547-551.
- 12. Foecke T, Lashmore DS, Scripta Metall. Mater. 1992;(27):651-656.
- 13. Handbook of Thermal Spray Technology, ASM International, Materials Park, OH, USA. 2004;171.
- 14. Ko PL, Robertson MF. Wear Characteristics of electrolytic hard chrome and thermal sprayed WC-10% Co-4% Cr coatings sliding against Al-Ni-Bronze in air at 21°C and at -40°C, Wear. 2002;(252):880-893.
- 15. Saharoui T, Fenineche NE, Montavon G, Coddet C. Alternative to chromium: characteristics and wear behaviour of HVOF coatings for gas turbine shafts repair (heavy-duty), J. Mater. Process. Technol. 2004;(152):43-55.
- 16. Rastegar F, Richardson DE. Alternative to chrome: HVOF cermet coatings for high horse power diesel engines, Surf. Coat. Technolo. 1997;(90):156-193.
- 17. Gieger G. Ceramic coatings enhance material performance, Am. Ceramic Soc. Bull. 1992;71(10):1470-1481
- 18. Chen H, Lee SW, Hao Du, Chen X Ding, ChulHo Cho. Influence of feed stock and spraying parameters on the deposition efficiency and micro hardness of plasma sprayed Zirconia coatings; Materials Letter. 2004;58(7-8):1241-1245.
- 19. Lalleman-Tallaron G. Study of Microstructure and adhesion of spineless coatings formed by plasma spraying, PhD Thesis, Thesis no. 96-58, E.C. Lyon, France; 1996.
- 20. Sutar H, Mishra SC, Sahoo SK, Satapathy A, Kumar V. Morphology and solid particle erosion wear behavior of red mud composite coatings. Natural Science. 2012;4(11):832-838. doi: 10.4236/ns.2012.411111.
- 21. Prasad N, Sutar H, Mishra SC, Sahoo SK, Acharya SK. Dry sliding wear behavior of aluminium matrix composite using red mud an industrial waste; International Research J of pure and applied chemistry. 2013;3(1):59-74.

© 2013 Satapathy et al.; This is an Open Access article distributed under the terms of the Creative Commons Attribution License (http://creativecommons.org/licenses/by/3.0), which permits unrestricted use, distribution, and reproduction in any medium, provided the original work is properly cited.

Peer-review history:

The peer review history for this paper can be accessed here: http://www.sciencedomain.org/review-history.php?iid=202&id=16&aid=1157